$In_xZn_{1-x}O$ 나노구조의 합성

정미나*, 하선여*, 이홍찬*', 이상태*', 조영래**, 고항주***, 김정진****, Y. Murakami*****, T. Yao*****', 장지호*

*한국해양대학교 반도체물리전공 대학원, *'한국해양대학교 선박기계공학부 교수

**부산대학교 재료공학부 교수, ***한국광기술원, 물성분석센터 센터장

**** 일본고휘도광과학연구센터 공학박사

***** 동북대학교 금속재료연구소 기술부 *****' 동북대학교 금속재료연구소 응용물리학 교수

Synthesis of $In_xZn_{1-x}O$ nanostructures

M. N. Jung, S. Y. Ha*, H. C. Lee*', S. T. Lee*', Y. R. Cho**, H. J. Ko***, J. J. Kim****, Y. Murakami*****, T. Yao*****', and J. H. Chang**

**Major of Semiconductor Physics, *'Department of Mechatronics Engineering, Korea Maritime University, Busan 606-791, Korea*

***Materials Science and Engineering, Pusan National University, Busan 609-735, Korea*

****Korea Photonic Technology Institute, Gwangju 500-460, Korea*

*****Japan Synchrotron Radiation Research Institute, 1-1-1 Kouto, Sayo-cho, Sayo-gun, Hyogo, 679-5198, Japan*

******Institute for Materials Research, Technical Services Division, *****' Tohoku University 2-1-1 Katahira, Aoba-ku, Sendai, 980-8577, Japan*

요 약 : 인듐의 서로 다른 함량에 다양한 $In_xZn_{1-x}O$ 나노 구조에 대한 합성과 구조적인 분석에 대해 알아보았다. 순수한 tetrapod 형 ZnO 나노 구조는 100-200 nm, 1-2 ㎛의 직경과 길이를 가지고 있지만, 인듐의 함량을 증가시킬수록 나노 구조의 모양은 불규칙적인 멀티포드형 층상구조를 갖는다. 가장 많은 인듐 함량을 가진 InZnO 나노 구조는 팔면체형 나노 구조와 마이크로단위의 크기를 갖는다. 이런 층상구조의 원인은 인듐의 불균일성에 의해 생각된다. 발광특성 또한 인듐이 많이 들어간 샘플일수록 UV 발광 피크가 red -shift 경향을 보이고 이는 직접천이에서 간접천이로의 밴드갭 이동으로 간주된다.

핵심용어 : InZnO, 나노구조, 인듐 조성, SEM, PL

ABSTRACT : *Systematic investigations on the synthesis and morphological variation of $In_xZn_{1-x}O$ nanostructures ($0 < x < 0.6$) have been studied. The pure ZnO tetrapod structures have four legs with a diameter of 100 - 200 nm and length of 1 - 2 ㎛, while with indium-content increasing, the significant variations of the shape as well as the size of nanostructure were observed. At the lowest In-content range ($x < 6$ %), multipod structures appeared, while it becomes an irregular multipod with a modulated*

facet structure at low In-content range (a few < x < 30 %), and finally octahedrons with a diameter of 500 nm ~ 1㎛ were observed at the highest In-content (x ~ 60 %). The origin of the modulated facet structure, looks like a stacked layer structure, is discussed in terms of the relaxation of strain due to inhomogeneous distribution of In-atoms. The red-shift of UV emission peak (from 3.28 eV to 3.20 eV with indium-content increasing 0 to 30 %), is tentatively attributed to the direct to indirect band gap transition.

KEY WORDS : InZnO, Nanostructure, Indium composition, SEM, PL

1.Introduction

Metal-oxide nanostructure is attracting the great interest for its potential applications to the nano-device and nano-technology[1]. Up to now, nanostructures of pure metal-oxides, such as ZnO[2], CdO[3], SnO[4], and In_2O_3,[5] have been successfully fabricated by using various methods[6]-[8]. Among the various metal oxides, ZnO is one of the most intensively studied materials due to the unique physical properties such as large exciton binding energy (60 meV) and direct wide band gap (3.44 eV at 0 K).[9] Therefore, a lot of studies have been performed on the growth, characterization, and device application of ZnO. Also, to tailor the electrical properties of ZnO for the specific applications such as transparency-conducting film and field emitter, several impurities such as Al, Ga, Sn, and In are introduced[10]-[13]. Among them, InZnO (Indium Zinc Oxide) attracts many interests for the application to the transparency-conducting electrode. InZnO thin films have low resistivity, high transmittance in the visible region, and high quality films can be easily obtained by using various simple methods, such as pyrosol process, sputtering, and metal-organic chemical vapor deposition (MOCVD)[14][15]. Particularly, InZnO thin films show similar electrical conductivity and better transparency in comparison to the ITO (indium-tin-oxides) films in the visible and infrared spectral range[16]. Therefore, a lot of reports on the structural, electrical, and optical properties of InZnO films are already available.[17-19] However, although unique physical properties are expected from the nanostructure version of this novel material, the synthesis and the characterization of InZnO nanostructures have been in the primitive stages so far. Moreover, the metal-oxide nanostructures have various shapes along with the growth conditions, thus it is important to know the variation of shape, structural and optical properties of InZnO depending on the In-content to utilize the specific feature of InZnO nanostructures. In this work, InZnO nanostructures with various In-contents were grown by the vapor phase transportation method. And systematic investigations on the morphological variation of $In_xZn_{1-x}O$ nanostructures ($0 < x < 0.6$) have been studied.

2.Experimental

InZnO nanostructures were grown by the vapor phase transportation method. To

make the InZnO nanostructure with different indium composition at atmospheric pressure, the mixture of each element (indium and Zn powder) was used as a source material, which was placed in the specially designed quartz tray. The tray was positioned at the center of the horizontal tube furnace. The growth of InZnO nanostructures was performed at 950 ℃ under the nitrogen gas flow. The variation of shape and dimension of the InZnO nanostructures were observed by scanning electron microscopy (SEM). The In-content of InZnO product was measured by auger electron spectroscopy (AES) and transmission electron microscopy (TEM). And the photoluminescence (PL) spectroscopy was performed by using a He-Cd laser (325 *nm*) as an excitation source, and a monochromator with a focal length of 32 cm at room temperature.

3. Results and discussion

Fig. 1 shows the SEM images of $In_xZn_{1-x}O$ ($0 < x < 0.6$) nanostructures. Various morphologies from tetrapod to octahedron were observed. Fig. 1(a) is the pure ZnO tetrapod structure. As listed in the table 1, the tetrapod structure shows 1 ~ 2 ㎛ long hexagonal legs with a diameter of 100 ~ 200 nm. However, when we mixed indium into the source material, the shape of the product became the multipod as shown in the Fig. 1(b). AES investigation shows the In-composition of the products is ~ 6 %. Remarkable elongation of the branch length is observed. Also, over-growth in the center region (marked with the arrows in the Fig. 1 (b)), and the distortion of inter-leg angles were found. The tetrapod-type ZnO nanostructures are known to have an inter-leg angle ~ 109 ° following the octa-twinning model.[20][21]But it might be changed by the incorporation of impurities and crystal defects, also the formation of multipod would be enhanced. Therefore the variation of inter-leg angle and over-growth at the

Table 1 The dimensions of $In_xZn_{1-x}O$ ($0<x<0.6$) nanostructures

Specimen	ZnO	$In_{0.06}Zn_{0.94}O$	$In_{0.15}Zn_{0.85}O$	$In_{0.6}Zn_{0.4}O$
Shape	Tetrapod	Multipod	Layered -Multipod	Octahedral -island
Diameter (nm)	100-200	200-300	1500-2000	500-1000
Length (㎛)	1-2	2-5	5-8	*

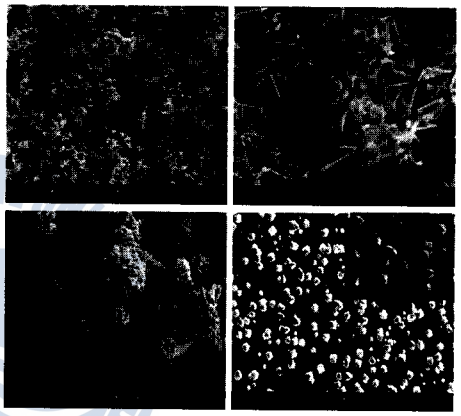

Fig.1 SEM images (a) pure ZnO nano structure, (b) $In_{0.06}Zn_{0.94}O$ nano structure, (c) $In_{0.15}Zn_{0.85}O$ nano structure, and (d) $In_{0.6}Zn_{0.4}O$ nano structure and the inset of (d) is the magnified image of island.

center region can be attributed to the introduction of In-atoms and increase of defect induced by In-incorporation. More detailed discussions on the distortion of inter-leg angle will be presented elsewhere. Fig. 1(c) shows a SEM image of $In_{0.15}Zn_{0.85}O$ sample. It has the mutational morphologies. The thick legs appeared to be formed by the stacking of many polynomial discs with the different diameters. It may indicate that the strain distribution in the leg would be non-uniform in vertical direction rather than in longitudinal direction. It was reported that InZnO nanostructure with relatively high In-content forms a longitudinal superlattice structure along with the growth direction consisted of InO layer and ZnO:In layers[22]. It is suggested that the formation of modulated structure is closely related with the minimization of structural stress caused by the introduction of impurity atoms. Therefore, it seems that the inhomogeneous distribution of In-atoms is responsible for the observed mutational morphology in the nanostructure and will be discussed further by using the TEM results. The $In_{0.6}Zn_{0.4}O$ sample shows the octahedral-type island structure as shown in the fig.1(d). The inset of the fig.1(d) shows a magnified image of a typical island. It was reported that the InZnO thin films, deposited onto the glass substrates by using combinatorial techniques, show amorphous phase when the In-content is in between 45 ~ 80 %. Also the low In-content films (x < 45%) have a ZnO-like structure and the high In-content films have In_2O_3-like structure[19]. Therefore, the octahedral-shape island structure is deduced that the crystal structure of InZnO starts to be changed In_2O_3-like one. Fig. 2 shows the TEM results of $In_xZn_{1-x}O$ (x = 0 %, x ~ 30 %) nanostructures. Fig. 2(a) is the TEM image of ZnO tetrapod. Single crystalline defect-free four branches are observed. Also, the inset of fig. 2(a) shows the uniform hexagonal crystal structure aligned in c-axis direction. While, Fig. 2(b) shows a TEM image of $In_{0.3}$ $Zn_{0.7}O$ nanostructure. As already shown in the Fig. 1(c), the zigzag structure is observed at the edge region. Generally, the non-uniform contrast in a TEM image is known to be produced due to the thickness fluctuation and spatially inhomogeneous distribution of the atoms. In our experiment, since the thickness fluctuation was observed and the growth temperature was not high enough to grow a homogeneous material, it is valid to think the specimen has both effects and further investigation is required. The inset of fig.2(b) shows the selected area electron diffraction (SAED) pattern. In the SAED pattern, a series of small diffraction spots are shown in between two adjacent main spots, which indicates the periodic structure. It is well known that the period of ZnO:In layers between adjacent two InO layers plays an important role to determine the conductivity of InZnO film.[17] When thecompounds $In_2O_3(ZnO)_m$ (m=integer) has a distance d between two adjacent InO layers, a linear relationship between d and m is valid following the below equation.

$$d = 0.6349 + 0.2602\ m\ (\mathrm{nm}) \qquad (1)$$

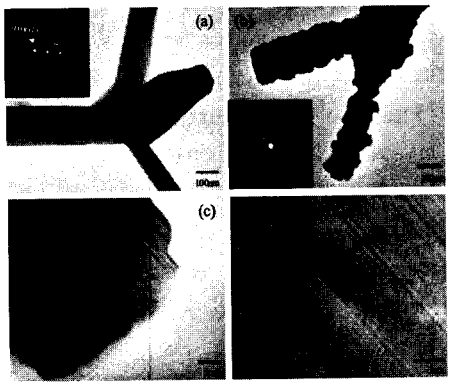

Fig. 2(a) TEM image of the ZnO tetrapod nanostructure and the inset of (a) is the selected area electron diffraction (SAED) pattern from the leg. Single crystalline hexagonal structure is observed, (b) TEM image of the $In_{0.3}Zn_{0.7}O$ nanostructure and the inset of (b) is the SAED pattern of periodic structure of InZnO indicates a superlattice-like periodic structure, (c) and (d) are high resolution image of the $In_{0.3}Zn_{0.7}O$ nanostructure shows a periodic structure consisted with ZnO:In and InO layers.

High-resolution images of $In_{0.3}Zn_{0.7}O$ are shown in Fig. 2(c) and (d). From those images, the inter-plane distance between two adjacent InO layers was measured. The average value of d is about 2.2 nm. Then m is calculated as ~ 6 by the equation (1). Thus the average composition of the nanostructure can be estimated as $In_2O_3(ZnO)_6$, which shows considerable correspondence with the compositions estimated from auger electron spectroscopy(~ 30%). The nominal inter-planner distance of ZnO:In is estimated to be 0.263 nm, however, it varies along with the longitudinal direction, presumably due to the inhomogeneity of indium-distribution. If the superlattice structure is formed due to the minimization of the structural stress, then the stress most presumably is introduced by the impurity atoms. It should be pointed that there was a report, which shows relationship between the superlattice period and morphology of the edge[23]. The authors argued that the superlattice period and morphology of the edge are closely related with the growth temperature. In general the sample grown at low temperature shows irregular edge structure period. And they concluded that long time annealing at high temperature will produce an ordered edge structure with uniform period. Although, more quantitative investigations are required to get a conclusion of this phenomenon, note that a large structural stress would be produced due to the difference of the tetrahedral covalent radii (In has 0.81, while Zn has 0.74)[22], and the crystallographic mismatch in between $In_2O_3$and ZnO:In. Moreover, especially when the growth temperature is not high enough to overcome the global minimization of the stress, it will relax locally and form the strongly modulated structure at the edge area. Therefore, in our experiment, both the relatively low growth temperature (950 °C) and high In-content are deduced for the strongly modulated structures at the facets. Fig. 3 shows room temperature PL spectra of $In_xZn_{1-x}O$ nanostructures. Fig. 3(a) is a PL spectrum of ZnO tetrapod structure. Note that only a weak green band

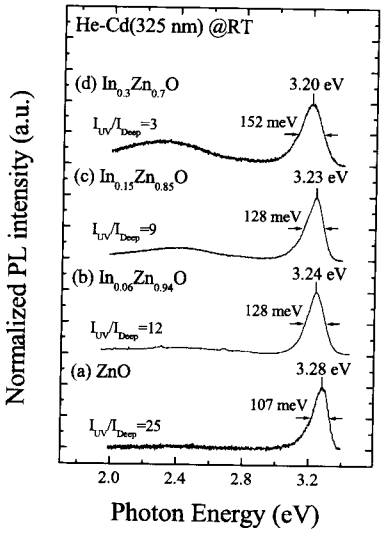

Fig. 3 Room temperature PL spectra of (a) ZnO nanostructure, (b) $In_{0.06}Zn_{0.94}O$ nanostructure, (c) $In_{0.15}Zn_{0.85}O$ nanostructure, and (d) $In_{0.3}Zn_{0.7}O$ nanostructure.

emission is observed until the In-content is as high as 30%. Usually, the tetrapod-type ZnO nanostructures, synthesized under various conditions, have strong green band emission centered at 2.45 ~ 2.5 eV[24]. The intensity of green band emission indicates the native defect density such as oxygen vacancy (V_O) and Zn interstitial (I_{Zn}) in the sample. However, we could not observe a luminescence at all from the $In_{0.6}Zn_{0.4}O$ sample. It is known that bulk InO is an indirect material at room temperature (direct band gap is 3.6 eV and indirect band gap is 2.6 eV)[25]. Although weak PL emission was reported from the InO nanowires (centered at ~ 2.64 eV)[26], the origin was attributed to the oxygen deficiency related emission. Therefore, the PL spectra are understood in terms of the recombination process changes from direct to indirect transition. Especially as In-content increases in the nanostructures, the degradation of crystallinity is observed in terms of the broadening of UV emission linewidth and increasing of the intensity ratio of UV emission to green emission due to the increase of crystallographic imperfections.

4. Conclusion

In this experimental, various InZnO nanostructures were synthesized by simple vapor phase transportation method. From the SEM images, the $In_xZn_{1-x}O$ ($0<x<0.6$) nanostructures with different In-contents exhibit the various shapes (tetrapod, layered hexahedron, and octahedron). In comparison with pure ZnO nanostructure, the InZnO nanostructures show a modulated edge structure related with the minimization of the structural stress originated by introducing indium. As indium-content increases, the recombination process changed from direct-to-indirect band gap transition.

Reference

[1] Y. R. Ryu, T. S. Lee, J. A. Lubguban, H.W. White, Y.S, Park, and C. J. Youn, Appl. Phys. Lett. 87 153504, 2005.

[2] M.H. Huang, Y. Wu, H. Feick, N. Tran, E. Weber, and P. Yang, Adv. Mater. 13 pp.113, 2001.

[3] Z. Ye, D. Ma, J. He, J. Huang, B. Zhao, X. Luo, and Z. Xu,J. Cryst. Growth 256

78, 2003.
[4] S. Budak, G.X. Miao, M. Ozdemir, K.B. Chetry, and A. Gupta, J. Cryst. Growth 291405, 2006.
[5] T. Gao and T. Wang, J. Cryst. Growth 290 660, 2006.
[6] S-W. Kim, S. Fujita, H-K. Park, B. Yang, H-K. Kim,and D.H. Yoon, J. Cryst. Growth pp.292 ~ 306, 2006.
[7] Y. Li, G.W. Meng, L.D. Zhang, and F. Phillipp, Appl. Phys. Lett. 76 2011, 2000.
[8] C.K. Xu, G.D. Xu, Y. Liu, and G. Wang, Solid State Commun. pp.122 ~ 175, 2002
[9] A.B. Djurisic and Y.H. Leung, Small XX. 1, to be published, 2006
[10] X-T, Hao, L-W. Tan, K-S. Ong, and F. Zhu, J. Cryst. Growth 287 44, 2006.
[11] C. Xu, M. Kim, J. Chun, and D. Kim, Appl. Phys, Lett. 86 133107, 2005.
[12] Z, Li, X. Li, X. Zhang, and Y. Qian, J. Cryst. Growth 291 258, 2006
[13] S.Y. Bae, H.C. Choi, C.W. Na, and J. Park, Appl. Phys. Lett. 86 033102, 2005.
[14] M-P. Taylor, D-W. Readey, C-W. Teplin, M-F.A. M. van Hest, J.L. Alleman, M.S. Dabney, L.M. Gedvilas, B.M. Keyes, B. To, P-A. Parilla, J.D. Perkins, D.S. Ginley, Macromol. Rapid Commun. 25 344, 2004.
[15] T. Moriga, A. Fukushima, Y. Tominari, S. Hosokawa, I. Nakabayashi, and K. Tominaga, J. Synchrotron Rad. 8 785, 2001.
[16] A. Wang, J. Dai, J. Cheng, M-P. Chudzik, T-J. Marks, R-P.h. Chang, and C-R. Kannewurf, Appl. Phys. Lett. 73 327, 1998.
[17] T. Minami, Semicond. Sci. Technol. 20 S35, 2005.
[18] P-M-R. Kumar, C-S. Kartha, K-P. Vijayakumar, T. Abe, Y. Kashiwaba, F. Singh and D. K. Avasthi, Semicond. Sci. Technol. 20 120, 2005.
[19] M-P. Taylor, D-W. Readey, C-W. Teplin, M-F.A. M. van Hest, J.L. Alleman, M.S. Dabney, L.M. Gedvilas, B.M. Keyes, B. To, J.D. Perkins, and D.S.Ginley, Meas. Sci. Technol. 16 90, 2005.
[20] H. Iwanaga, M. Fujii, and S. Takeuchi, J. Cryst. Growth 134 275, 1993.
[21] C. Ronning, N. G. Shang, I. Gerhards, H. Hofsass, and M. Seibt, J. Appl. Phys. 98 034307, 2005.
[22] J. Jie, G. Wang, X. Han, and J.G. Hou, J. Phys. Chem. B 108 17027, 2004.
[23] C. Li, Y. Bando and M. Nakamura, C. Li, Y. Bando, M. Nakamura, M. Onoda, and N. Kimizuka, J. Solid State Chem. 139 347, 1998.
[24] N.O. Korsunska, L.V. Borkovska, B.M. Bulakh, L.Y. Khomenkova, V.I. Kushnirenko and I.V. Markevich, J. Lumin. 102 733, 2003.
[25] X.S. Peng, G.W. Meng, J. Zhang, X.F. Wang, Y.W. Wang, C.Z. Wang, and N.D. Zhang, J. Mater. Chem. 12 1602, 2002.
[26] C. Liang, G. Meng, Y. Lei, F. Phillipp, and L. Zhang, Adv. Mater. 13 1330, 2001.

Received : 4 January 2007
Accepted : 24 January 2007